

# Analyses of Eddy-Current Losses and Levitation Force inside Induction Furnace by 3D Edge Finite Element Method

Vlatko Čingoski<sup>†</sup> Hideo Yamashita<sup>†</sup> Tatsufumi Aoi<sup>‡</sup>

<sup>†</sup>Faculty of Engineering, Hiroshima University, Kagamiyama 1-4-1, Higashihiroshima, 724 JAPAN

<sup>‡</sup>Mitsubishi Heavy Industry, Hiroshima, JAPAN

**ABSTRACT** – To optimize the shape and parameters and to increase efficiency of induction heating furnace, detailed simulation of its electromagnetic behavior is needed. Due to the complexity of the model, a special 3D edge finite element method (EFEM) with vector potential formulation and extended use of radial and axial symmetry was developed, enabling sufficient analysis based only upon a small slice of the model. We analyzed several models with different coil positions, number and position of cold crucibles and air-gap widths. Also, different values of frequency and intensity of the source current were considered in order to determine their influence over eddy-current losses and levitation force acting on the molten metal. In this paper the method of analysis, models and obtained results, which agree well with measured results are presented.

## I. INTRODUCTION

Induction heating furnaces are rather complex 3D electromagnetic devices, the optimization of which requires much computational time and cost. The recently developed EFEM with its short computation time, small memory requirements and satisfaction of only proper continuity conditions across boundary planes between different magnetic materials [1] [2], has developed into an interesting solution for such complicated devices.

In this paper, the authors present a successful approach to the analysis of eddy-current losses and levitation forces, two main parameters in the design process. Analyzing models with different shapes, cold crucible positions and air-gap widths between them, altering the frequency and intensity of the source current, we performed a deep investigation of the connections and influence of all these parameters over distribution and intensity of levitation forces and eddy-current losses. By developing a special 3D EFEM code, which enables analysis to take place only if a small slice of the quasi axis-symmetrical model of the furnace is actually discretized into extremely fine mesh, the highly accurate analyses were performed with minimal computation effort and cost [3]. On the other side, the program code shows improvements in the computation time not only due to a reduced number of finite elements, but also due to its improved convergence rate. This convergence rate improvement is very important in the case of ungauged magnetic vector potential formulation of the problem that we employed in the analyses, and is mainly the result of an improvement in the satisfaction of the solenoidal character of the source current density vector  $\nabla \cdot \mathbf{J}_0 = 0$ .

## II. METHOD OF ANALYSIS

As mentioned before, in these analyses EFEM was employed for its useful properties such as small memory requirements, short computation time, and satisfaction of only proper continuity conditions across boundaries between different magnetic materials. In other words, EFEM does not impose any additional continuity conditions on the approximated field distribution, preserving its natural physical properties. This is an important factor in achieving fast and accurate analysis. Regarding eddy-current problems driven by high-frequency sources where the penetration depth of eddy-currents is extremely shallow, the development of very fine and dense division mesh is imperative to obtain results with acceptable accuracy. This leads to a large number of finite elements and, even using EFEM, problems such as long computation and lack of memory almost always arise. Fortunately, we are able to use the symmetry of the model, requiring the development of finite element mesh only for a minimum symmetrical area. This characteristic was employed and a special 3D EFEM program code was developed, enabling analysis to take place while only a minimum slice of the quasi axis-symmetrical model of the furnace was discretized into finite element mesh [3]. The development of this program code was possible because of the ease of assignment of boundary conditions on an arbitrary plane in EFEM, a process that can be summarized as follows:

- Assign zero value to all edges that belong to any boundary plane with Dirichlet boundary conditions, and
- Leave free (unassigned) all edges that belong to certain planes with Neumann boundary conditions.

Assignment of boundary conditions, therefore, can be executed in two steps: Extraction of all edges on a certain plane and assignment of appropriate boundary conditions (eventually leaving them unassigned). This simple procedure enables the easy analysis of any arbitrarily chosen symmetrical slice of the model. In Fig. 1, a typical 3D finite element mesh for one of the analyzed models is presented.

## III. ANALYZED MODELS AND OBTAINED RESULTS

Optimization of the shape, characteristics and performance of such a complicated 3D electromagnetic device as the induction furnace, certainly involves considerable computational time and effort. The number of analyzed models and changing parameters, therefore, is of primary importance. To achieve accurate results throughout the entire research, the obtained results for some models must be compared with measured results for the same model. The significance of this comparison is twofold: to verify

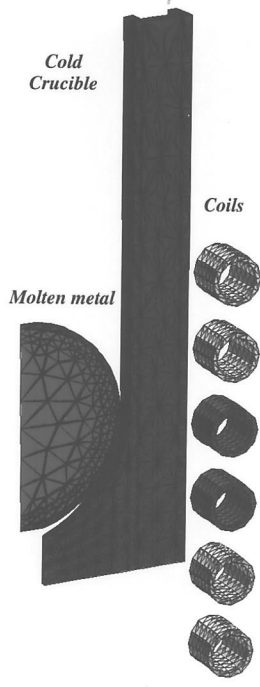


Fig. 1. 3D finite element mesh for the analysis region.

the software we use and to determine the approximated density of the finite element mesh for parts of the analyzed model as well as for the entire model to develop a mesh sufficiently dense for obtaining the desired accuracy.

Initially, from the main model presented in Fig. 2, two sub-models were analyzed. The main difference between the two sub-models was the length of the bases – the long base was 20 [mm] and the short base, 10 [mm]. Each of these two models was analyzed for three different coil positions:  $l = 0$  [mm],  $l = 30$  [mm], and  $l = 60$  [mm]. Also, different numbers of crucibles (8 and 16), with varying air-gap widths (1 [mm] and 2 [mm]) were considered. The analyses were performed for two discrete frequency values, 2000 [Hz] and 4000 [Hz], and for several source current intensity values in the range between 400 [A] and 1500 [A].

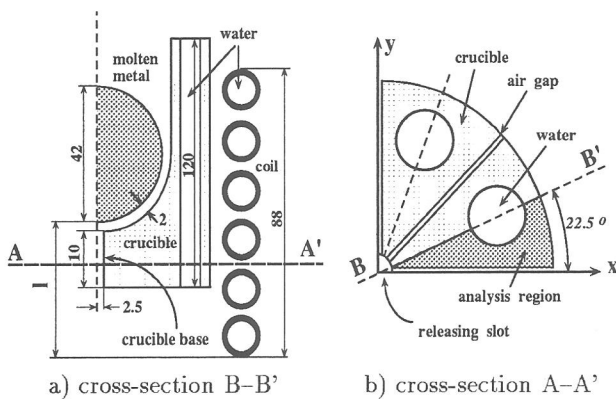


Fig. 2. Analyzed model of induction heating furnace.

Initially, the obtained results for magnetic flux density vector  $\mathbf{B}$  were compared with the measured values. The measured results were provided only for the inside area of the furnace without molten metal. The appropriate analysis was performed and the obtained results are presented in Fig. 3. Since the computational results agree with the measured results, we proceeded with analyses of eddy-current density distribution and eddy-current losses. In Fig. 4 a typical magnetic flux density and eddy-current distributions for one model are presented. The eddy current losses were computed separately for molten metal and for the cold crucible in order to find their relations and influence on the power efficiency of the furnace. Total eddy-current losses were computed using the Gaussian integration procedure with five integration points in each finite element

$$W = \sum_{i=1}^{nel} \left( \sum_{j=1}^5 w_j \frac{1}{\sigma_i} \mathbf{J}_{ej} \cdot \mathbf{J}_{ej}^* \right) V_i. \quad (1)$$

In the above equation  $nel$  is total number of elements in the conducting region (only molten metal or cold crucible),  $w_j$  is the weighted function for integration point  $j$ ,  $\mathbf{J}_{ei}$  and  $\mathbf{J}_{ei}^*$  are the values of the eddy-current density vector and its conjugate vector at each integration point inside the element, and  $V_i$  is the volume of finite element  $i$ .

Electromagnetic forces were computed using the *volume force density method*

$$F = \iiint_v \mathbf{J}_e^{Re} \times \mathbf{B}^{Re} dv, \quad (2)$$

where  $\mathbf{J}_e^{Re}$  and  $\mathbf{B}^{Re}$  are real parts of eddy-current density and magnetic flux density vectors, respectively. After integration of partial electromagnetic forces over the entire volume of molten metal, we can compute the levitation force acting on the molten metal inside the furnace. Since the shape of the molten metal is a sphere placed symmetrically inside the furnace, the direction of the radial components (x- and y-components) of electromagnetic force is toward the central axis and they cancel each other out. Therefore, only the z-component of the total force acting on the molten metal, i.e. the levitation force, has a significant meaning. Depending on the coil position, the air-gap widths, the diameter of the releasing slot under the molten metal and especially the length of the crucible base, the value of the levitation force can be regulated and controlled. In Fig. 5, a typical distribution of electromagnetic forces inside the molten metal is presented. Next, we will discuss the influence that different parameters have mainly on eddy current losses and levitation forces inside the furnace.

#### A. Coil position

The position of the coils around the furnace significantly influences eddy-current losses and, especially, levitation forces. Increasing the distance  $l$ , (see Fig. 2) increases the amount of levitation force and decreases the amount of energy consumed by the molten metal. Knowing the amount of molten metal inside the furnace and therefore its weight, makes it possible to find the optimal position of the coils so that the metal ball will actually levitate inside the furnace. For this analysis, we were able to compare the computed results with the measured results. The results agree very well as Fig. 6 demonstrates.

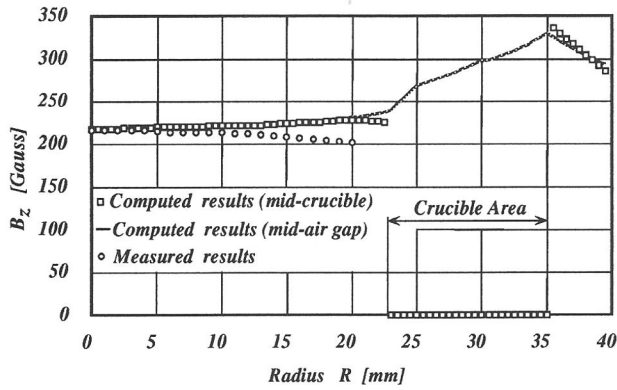


Fig. 3. Comparison between measured and computed results for z-component of magnetic flux density  $B_z$ .

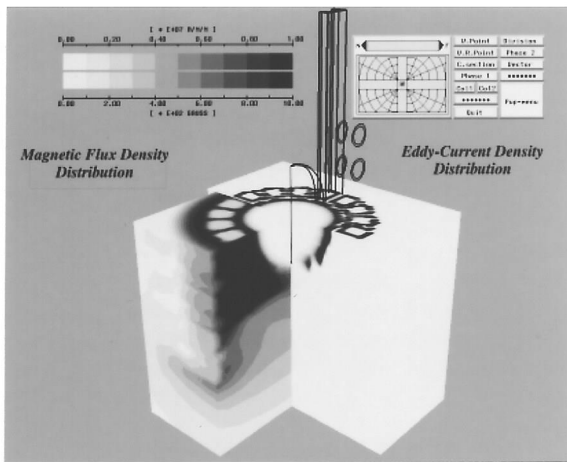


Fig. 4. Eddy-current and magnetic flux density distributions.

### B. Base lengths

The base of the cold crucible, besides its natural function of giving mechanical stability to the furnace, is at the same time a large consumer of power, and actually acts as a shield against the penetration of the magnetic flux inside the furnace. Decreasing its length, therefore, enables magnetic flux to flow freely inside the furnace which results in large amounts of used power and levitation force. Here, two different base lengths were considered: short (10 [mm]) and long (20 [mm]). The obtained results of the analyses with source current  $I_0 = 400$  [A], and frequency  $f = 2000$  [Hz] are presented in Table I. From Table I it is apparent that a short base is favorable for increasing the power efficiency of the furnace and for obtaining large levitation force.

### C. Source frequency

The influence of source frequency on the amount of eddy current losses and levitation force was also analyzed. The obtained results for the value of source current  $I_0 = 400$  [A] are presented in Table II. From the results it is evident that eddy current losses increase as the source

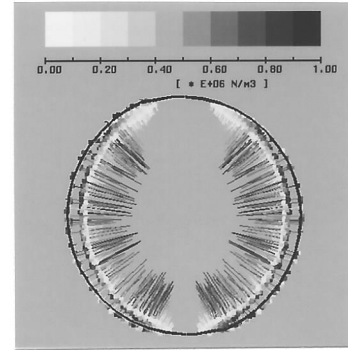


Fig. 5. Electromagnetic force distribution.

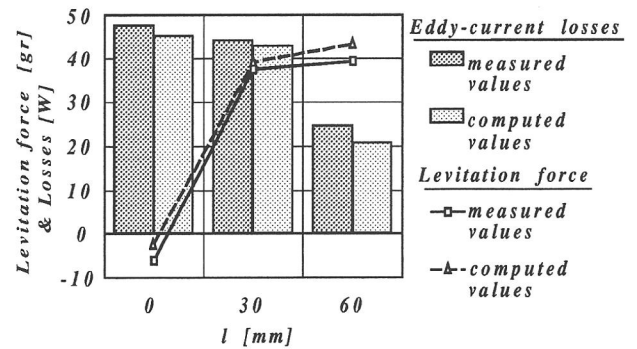


Fig. 6. Influence of coil position on eddy-current losses and levitation forces inside molten metal.

frequency increases. In terms of levitation force, the opposite trend can be observed. This is result, we believe, of the fact that in case of higher frequencies, the depth of the area of molten metal on which the electromagnetic forces act is very shallow, so in effect, we are actually computing a kind of surface force. In this case, the possibility of inaccurate results is high. Further proof is the fact that for higher frequencies the maximum force density vector is larger than that for lower frequencies. The total force obtained by volume integration (2), however, is smaller overall.

TABLE I.

*Eddy-current losses and levitation force vs. base length*

$l$ [mm]	Eddy current losses [W]			Levitation force [gr]		
	0	30	60	0	30	60
Long Crucible	45.32	42.89	20.82	-2.04	39.14	43.22
Short Crucible	48.98	47.30	23.49	4.89	48.52	49.34

### D. Number of crucibles and air gap width

During analyses, different numbers of cold crucibles and air-gap widths were also considered. The obtained results

for three different models are presented in Table III. Eddy-current losses in molten metal increase as the number of crucibles increases due to the increase in the number of air-gap slots between them. The eddy-current losses in cold crucibles also increase. However, an increase in the number of crucibles is favorable because it results in an increase in the power efficiency of the furnace. The number of crucibles has very little influence on the amount of levitation forces acting on molten metal.

TABLE II.

*Eddy-current losses and levitation force vs. source frequency*

$l$ [mm]	Eddy current losses [W]			Levitation force [gr]		
	0	30	60	0	30	60
2000 [Hz]	45.32	42.89	20.82	-2.04	39.14	43.22
4000 [Hz]	68.11	63.12	30.52	1.22	35.88	38.33

TABLE III.

*Eddy-current losses and levitation force vs. number of crucibles and air-gap widths*

Model	1	2	3
Number of crucibles	16	8	8
Air-gap [mm]	1	1	2
Base height [mm]	20	20	10
(1) Eddy-current losses in molten metal [W]	239.55	200.72	235.17
(2) Eddy-current losses in cold crucibles [W]	2468.09	1924.18	1623.94
$\frac{(1)}{(1)+(2)} \cdot 100[\%]$	8.84	9.45	12.65
Levitation force [gr]	256.57	258.47	302.68

$$I_0 = 1000.0 \sqrt{2} \cdot \sin(\omega t) [A]$$

$$f = 2000 [Hz]$$

#### E. Diameter of the releasing slot

Since the influence of the amount of source current on the eddy-current losses and levitation force is predictable and straightforward, the last point that we would like to discuss is the influence of the diameter of the releasing slot  $d$  of the furnace (in Fig. 2,  $d = 5$  [mm]). Again, three different models were considered with diameters  $d = 4$  [mm], 10 [mm] and 15 [mm]. The obtained results are presented in Table IV. From the results, increasing the releasing slot diameter results in:

- Large increase in the amount of levitation forces, and modest increase in eddy current losses,
- Increase in the power efficiency factor due to the increase of magnetic flux in the area of the releasing slot. This slot actually emphasizes the magnetic flux in this area.

As a reference, the complete analysis was performed using the *Silicon Graphics Indigo-Crimson* workstation with 64 Mbyte operating memory and 128 MIPS, and the total CPU time for one analysis and for model with 9343 points, 47076 finite elements, 59259 edges and 736232 non-zero entries in the matrix of the system was about 103 min.

TABLE IV.

*Eddy-current losses and levitation force vs. diameter of releasing slot  $d$*

$d$ [mm]	4	10	15
Number of crucibles	16	16	16
Air-gap [mm]	1	1	1
Base height [mm]	10	10	10
(1) Eddy-current losses in molten metal [W]	256.68	257.73	258.58
(2) Eddy-current losses in cold crucibles [W]	2198.89	2179.23	2149.09
$\frac{(1)}{(1)+(2)} \cdot 100[\%]$	10.45	10.58	10.74
Levitation force [gr]	292.75	300.72	306.91

$$I_0 = 1000.0 \sqrt{2} \cdot \sin(\omega t) [A]$$

$$f = 2000 [Hz]$$

#### IV. CONCLUSIONS

In this paper a successful method for the analysis and optimization of the shape and parameters of an induction heating furnace using 3D EFEM was presented. The influence of the number of crucibles, air-gap widths, shape of the furnace and also the position and parameters of the coils is great, and it is very important that it be considered in the process of analysis and especially design. Concerning the optimization parameters, in this analysis — eddy-current losses and levitation forces, it is possible to obtain optimal shape and parameters of the furnace. A modified 3D EFEM program code was developed in order to deal effectively with such intensive analysis. The obtained results agree with the measured ones, therefore the proposed method could be also favorable in the design and analysis of other induction heating devices.

#### REFERENCES

- [1] M. L. Barton, Z. J. Cendes: "New Vector Finite Elements for Three-dimensional Magnetic Field Computation," *J. Appl. Phys.* 61, (8), (15), pp. 3919 - 3921, April 1987.
- [2] K. Preis, I. Bardi, O. Biro, C. Magele, G. Vrisk, K. R. Richter: "Different Finite Element Formulations of 3D Magnetostatic Fields," *IEEE Trans. of Magn.* Vol. 28, No. 2, pp. 1056 - 1059, March 1992.
- [3] V. Čingoski, H. Yamashita: "An Improved 3-D Edge Finite Element Method for Eddy-Current Analysis of Induction Furnace Using Sliced Models," *ISEM - 94, June 22-24*, Seoul, 1994.